Water Practice & Technology

IWA PUBLISHING

Water Practice & Technology Vol 19 No 8, 2973 doi: 10.2166/wpt.2024.140

Adsorption of azithromycin antibiotic from water onto biochar derived from *Terminalia chebula* and sugarcane bagasse

Mrinal Patil[a], Sangeeta Singh[a], Divyani Kumari[a], Achlesh Daverey[b] and Kasturi Dutta [a,*]

[a] Department of Biotechnology and Medical Engineering, National Institute of Technology, Rourkela, Odisha 769008, India
[b] School of Environment and Natural Resources, Doon University, Dehradun, Uttarakhand 248012, India
*Corresponding author. E-mail: duttakasturi@nitrkl.ac.in

KD, 0000-0001-7233-41550000-0001-7233-4155

ABSTRACT

In the present study, *Terminalia chebula* biomass was utilized to produce biochar. *T. chebula*-derived biochar (CBC) was characterized, evaluated as an adsorbent to remove azithromycin from the water, and compared with sugarcane bagasse-derived biochar (BBC). The effects of different environmental parameters on the adsorption capacity of the biochar were studied by response surface methodology. The adsorption for CBC after optimization increased by 43.65%, and for BBC it increased by 51.99%. The maximum adsorption capacities (q_m) for CBC and BBC were found to be 21.36 and 17.95 mg/g, respectively. Various adsorption isotherm models were also studied to confirm the adsorption capacity. The results suggest that the Langmuir model fitted best among the tested models with respect to high correlation coefficients in both cases (R^2, 0.886 for CBC and 0.872 for BBC). The nonlinear pseudo-first-order kinetics was a better fit for the adsorption experiment data in both cases. Furthermore, it can be concluded that both CBC and BBC are fairly effective in treating wastewater with high antibiotic content after optimization.

Key words: adsorption kinetics, agro-industrial waste, emerging contaminants, response surface methodology, waste valorization

HIGHLIGHTS

- *Terminalia chebula* biomass and sugarcane bagasse were valorized as biochars (CBC and BBC) for the adsorptive removal of azithromycin from water.
- The process parameters for the adsorption of azithromycin on the biochar were optimized using RSM.
- The q_m for CBC and BBC were found to be 21.36 and 17.95 mg/g, respectively.
- The adsorption followed the Langmuir isotherm model.

ABBREVIATIONS

AMR antimicrobial resistance
BBC bagasse-derived biochar
CBC *T. chebula*-derived biochar
CCD central composite design
EDS energy dispersive X-ray spectroscopy
FTIR Fourier transform infrared spectroscopy
RSM response surface methodology
SEM scanning electron microscopy
XRD X-ray diffraction

1. INTRODUCTION

Antimicrobial resistance (AMR) is a serious concern of the 21st century that threatens the public health care system. AMR has effectively harmed the treatment and prevention of emerging microbial infections. Microbes are no longer susceptible to the common medicines used for their treatment (Peng *et al.* 2022). The World Health Organization declared the coronavirus outbreak in 2019 brought on by the SARS-CoV-2 virus as a pandemic on March 11, 2020. This outbreak reshaped the global public health concern about AMR as there is

rampant use of antibiotics. It is well known that a major portion of the antibiotics consumed by humans (and animals) are not completely metabolized by their bodies. Unmetabolized antibiotics are let into the soil and water by various means, such as municipal wastewater, animal manure, sewage sludge, and biosolids. These increased concentrations of antibiotics in the environment have led to the emergence of much higher levels of AMR. AMR occurs when microorganisms, including bacteria, fungi, parasites, and viruses, develop resistance against the medicinal drug that once affected them due to excess exposure (Dadgostar 2019). It is estimated that in the USA, AMR organisms cause about 2 million infections, which lead to approximately 23,000 deaths per year (Marston *et al.* 2016).

Azithromycin, a broad-spectrum antibiotic, has been licensed for the treatment of respiratory infections, otitis media, skin infections, and sexually transmitted diseases (Koch *et al.* 2005). With the COVID-19 pandemic, the use of azithromycin as a treatment increased. The human body does not completely metabolize azithromycin, and a sizeable amount is added to wastewater treatment facilities. Furthermore, azithromycin has a slow metabolism, indicating poor degradation in aqueous medium and resulting in higher levels in the environment (Koch *et al.* 2005).

Antibiotics have been removed using a variety of biological and physicochemical approaches (Xu *et al.* 2020). Several advanced technologies such as photocatalytic degradation chemical oxidation via ozone or ozone/hydrogen peroxide, electrochemical treatments, membrane filtration techniques (such as nanofiltration and reverse osmosis), surface adsorption onto the carbonaceous adsorbents or nanomagnetic adsorbents have been investigated in recent years to remove these pollutants. However, due to the advantages of adsorbent such as simplicity, low toxicity, cheap energy cost, and high removal effectiveness, adsorption is accepted widely (Xu *et al.* 2020). Many absorbents, such as resin, bentonite, activated carbon (Shao *et al.* 2021), zeolite, chitosan, carbon nanotubes (Xu *et al.* 2020), and biochar are used for the removal of contaminants. Biochar, produced by pyrolysis under oxygen-deficient conditions, is a carbon-rich material (Pan 2020). It is generally produced from organic wastes such as agriculture waste, municipal sewage waste, forest residue, and animal manure. Biochar possesses enhanced properties such as a large surface area, higher cation and anion exchange capacities, and a stable structure. Biochar is preferable to biomass because it increases carbon sequestration, reduces waste, and emits less greenhouse emissions. Lignocellulosic biomasses such as agro-industrial wastes and forest wastes are the preferred raw materials for the preparation of biochar due to their low-cost and abundance (Pandey *et al.* 2020). Biochar derived from various sources, such as oak wood, paper mill sludge (Masrura *et al.* 2022), rice husk (Herrera *et al.* 2022), wood chips (Muter *et al.* 2019), etc., have been used for the adsorptive removal of azithromycin from the water. Herrera *et al.* (2022), utilized rice husk biochar to remove azithromycin up to 200 mg/L, with a removal efficiency of 95%. Chen *et al.* (2019), have found to have maximum removal efficiency of 85.1% for azithromycin with biochar derived from spent mushroom substrate.

Terminalia chebula is a species of *Terminalia* that is also known as Black Myrobalan or Harrad. It is widely distributed throughout India, Nepal, China, Sri Lanka, Malaysia, and Vietnam (Nallathambi *et al.* 2022). *T. chebula* is a flowering and medicinal plant widely used in ayurvedic medicine to treat various diseases. While sugarcane bagasse is one of the most abundantly available agro-industrial wastes and has been widely explored for the production of biochar (Iwuozor *et al.* 2022). Sugarcane bagasse biochar has been used for the removal of antibiotics like sulfonamide, tetracyclines, and other contaminants like carbofuran (Jacob *et al.* 2020). However, the removal of azithromycin by adsorption using sugarcane bagasse biochar and *T. chebula* biochar has not yet been investigated.

The aim of the study was to utilize *T. chebula* and sugarcane bagasse for the development of biosorbent for the adsorptive removal of azithromycin from wastewater. Biochar was characterized by SEM, FTIR, and XRD. Along with adsorbent dosage, temperature and pH were also investigated. Furthermore, isotherms, kinetics, and thermodynamic studies were also executed to understand the underlying mechanism of adsorptive removal of azithromycin from wastewater through both biochars.

2. MATERIALS AND METHODS

2.1. Materials

The fruits of *T. chebula* were collected from the garden of the NIT Rourkela Campus, while sugarcane bagasse was collected from the cane juice vendor on the NIT Rourkela Campus. Azithromycin for injection, USP 500 mg – Ozitop (Oscar Remedies Pvt. Ltd) was purchased from the Community Welfare Society Hospital (CWS

Hospital) in Rourkela. A concentration of 25,000 mg/mL was achieved by dissolving 500 mg of azithromycin in 20 mL of 0.01 M phosphate buffer with a pH of 7.5. This solution was prepared due to the compound's low solubility in water and the isotonic conditions maintained by phosphate buffer (Mangal *et al.*, 2018). A homogenized solution was generated due to its high solubility in phosphate buffer. Subsequently, a homogenized solution was diluted using distilled water. All other chemicals were purchased from Himedia.

2.2. Estimation of azithromycin concentration by spectrophotometric method

A stock solution (250,000 mg/L) of azithromycin was prepared from which a working solution of 1,000 mg/L was obtained by diluting with distilled water. The working solution of azithromycin (1,000 mg/L) was further diluted with distilled water to get final concentrations of 100, 150, 200, 250, 300, and 400 mg/L for standard curve preparation. For the estimation of azithromycin, water samples were treated with 9 mL of 13.5 M sulfuric acid and heated in a water bath at 50 °C for 30 min. Through this reaction, the antibiotic undergoes hydrolytic cleavage of the glycosidic linkage and generates an erythronolide aglycone moiety. This reaction results in the formation of erythronolide, a yellow compound that exhibits intense adsorption. The samples were cooled down at room temperature and then absorbance was taken at 482 nm by a UV-Vis spectrophotometer (Double beam spectrophotometer 2203 Systronic) as reported earlier (Kumar *et al.* 2013).

2.3. Biochar preparation

Rigorous cleaning was performed on the bagasse and *T. chebula* (Figure 1). *T. chebula* fruits were left to air dry for 4 h. After the fruits were cleaned and air dried, they were peeled to remove the mesocarp. The bagasse was shredded into tiny pieces and the fruits were rinsed three times with tap water for 2 h to remove any remaining dirt. A hot air oven was used to dry the *T. chebula* mesocarp for 72 h at 70 °C, while the cleaned bagasse was dried for 36 h at the same temperature. Next, an electric grinder was used to reduce the size of dry bagasse and *T. chebula* mesocarp to a coarse powder. The biomass was preserved in an airtight container after the pulverized powder was passed through a 1.18 mm filter. In a muffle furnace with oxygen levels controlled, the biomass was heated to pyrolysis. The biomass was heated in a closed crucible at 500 °C for 1 h at a rate of 5 °C/min in order to produce biochar, bagasse (BBC) and *T. chebula* (CBC). After cooling, the biochar was washed extensively with distilled water and then dried in a hot air oven at 70 °C for 12 h. The dried biochar was sealed in a container for further usage.

Figure 1 | (a) Fruit of *T. chebula*, (b) seed of *T. chebula*, (c) mesocarp of *T. chebula*.

2.4. Biochar characterization

Various analytical methods were utilized to characterize the biochar. For pH analysis, 1 g of biochar was added to 50 mL of distilled water. The pH was taken using a pH meter after 30 min (Pandey *et al.*, 2022a). The amounts of moisture, volatile matter, ash, and fixed carbon were all calculated using proximate analysis. The morphology and structure of the biochar were analyzed by SEM (Scanning Electron Microscopy) (JEOL JSM-6480 model, Jeol USA Inc., Peabody, MA, USA), with EDS (Energy Dispersive X-ray Spectroscopy). The nitrogen adsorption/desorption isotherms of the biochar were characterized at –196.15 °C by using a surface area and porosity analyzer to obtain the BET-specific surface area and pore size. The functional groups of biochar were determined using

Fourier Transform Infrared Spectroscopy (FTIR) (Alpha ATR-FTIR, Bruker, USA) in the 500–4,000 per cm range. X-ray diffraction (XRD) was used to identify the crystalline phase and its ratio with the amorphous phase of the biochar. *T. chebula* and sugarcane bagasse biochar were analyzed using the following operating parameters: with a step size of 7°, the 2θ angle measurement range was adjusted from 0° to 80° (Kwoczynski & Čmelík 2021).

The point of zero charge (pzc) determination study was performed using 0.3 g of biochar in 50 mL of 0.1 M NaCl. The pH of solutions was adjusted to acidic values ranging from 2 to 6 using HCl, while the alkaline pH was adjusted from 8 to 12 using NaOH. The mixtures were equilibrated in a rotatory shaker at 160 rpm for 24 h at room temperature. Using a pH meter, the ultimate pH was subsequently determined. The pH value of ΔpH was graphed against the initial pH, with the point at which the graph intersected the x-axis, which represented the point of zero charge. The ΔpH was calculated using Equation (1) (Tran *et al.* 2016):

$$\Delta\text{pH} = \text{Final pH} - \text{Initial pH} \tag{1}$$

2.5. Adsorption studies

Adsorption studies were carried out to better understand the adsorption capabilities of the produced biochar. To understand the time required to reach the adsorption equilibrium, batch adsorption studies with azithromycin concentrations of 200 mg/L and biochar dosages of 200 mg, pH 7 and 30 °C were carried out. Optimization studies were carried out by fixing the azithromycin concentration to 200 mg/L and 50 mL volume in a 250 mL conical flask and keeping it in a shaking incubator at 160 rpm for 120 min to understand the effect of biochar dosage, pH, and temperature. Central composite design (CCD) was used as an optimization tool in response surface methodology (RSM) to understand the impact of the independent process variables on the adsorption process. Three process variables, biochar dosage, pH of azithromycin solution, and temperature, were investigated. Using the equation obtained from the standard curve for azithromycin, the concentration of the solution after adsorption was estimated. The percent azithromycin removal was evaluated using Equation (2), where C_0 implies the initial concentration of azithromycin (mg/L), and C_t implies the azithromycin concentration (mg/L) at any time t. All experiments were performed in duplicate. The experimental data obtained were studied by means of Minitab's software:

$$\%\ \text{Removal} = \frac{C_0 - C_t}{C_0} \times 100 \tag{2}$$

2.6. Adsorption kinetics and thermodynamics

Kinetics were performed using 50 mL initial concentrations of 100, 150, 200, 250, 300, 350, and 400 mg/L of azithromycin solution. The optimized conditions for CBC were 0.35 g of biochar, pH of 8.47 and 37.5 °C temperature, whereas for BBC were 4.7 gm of biochar, pH 10.19, and 38.7 °C temperature. The flasks were incubated in a shaking incubator at 160 rpm for 180 min. Similarly, a thermodynamic study was performed at three different temperatures 29.9, 37.3, and 43.9 °C and at a constant initial concentration of azithromycin (Lagergren 1898; William Kajumba *et al.* 2019).

2.7. Adsorption isotherm studies

The maximum adsorption capacities (q_e, mg/g) of the biochar and the mechanism involved in the adsorption of azithromycin on biochar were understood by conducting adsorption isotherm studies. Data from the kinetics study were used to fit the isotherm models (Langmuir 1919; Mahecha-Rivas *et al.* 2021; Saldarriaga *et al.* 2021):

$$q_e = (C_0 - C_e)\frac{V}{m} \tag{3}$$

Here, q_e is maximum adsorption capacity, C_0 is the initial concentration of azithromycin (mg/L), C_e is the final concentration of the azithromycin (mg/L), V is the volume of the solution (L) and m is the mass of the adsorbent (g).

2.8. Reusability of CBC and BBC

The reusability study of CBC and BBC was carried out by the following method. For adsorption, 0.3 g of biochar sample (CBC or BBC) was mixed with 100 mg/L azithromycin and the solution was incubated for 24 h at 25 °C in

an orbital shaker. After 24 h of incubation, the samples were collected and filtered using a vacuum filtering device. Desorption was conducted for a duration of 24 h using 25 mL of desorption solution (0.05 M NaOH for CBC and 0.1 M HCl for BBC) on the filtered biochar. After desorption, the samples were collected and subsequently filtered through a vacuum filtration apparatus. The collected supernatants were used for the estimation of azithromycin. The filtered biochar was then air-dried at room temperature and used for adsorption again. The cycle was repeated three times (Mdlalose 2018).

3. RESULTS AND DISCUSSION

3.1. Characterization of biochar

The textural characteristics of CBC and BBC are present in Table 1. The pH of both the biochar was slightly acidic to neutral, with CBC having a pH value of 6.84 and BBC having a pH value of 6.94. It has been observed that biochar produced with low ash content generally has a lower pH as compared to biochar produced with high ash content (Singh *et al.* 2017). Also, the pH is higher at pyrolysis temperatures above 400 °C than at temperatures below 400 °C, as of this study (Sharma *et al.* 2012). After adsorption pH of BBC changed to 7.85, while for CBC, it was 6.80. The point of zero charge, which is the pH at which the net surface charge on the adsorbent is zero, was found to be 5.25 for CBC and 7.73 for BBC (Supplementary material, Figure S1). At this pH, the biochar was in an equilibrium state. The proximate analysis and elemental contents of the two biochars (CBC and BBC) are compared in Table 1. The yield and fixed carbon of CBC were higher than those of BBC.

Table 1 | Proximate analysis and elemental contents of biochar

Proximate parameter	CBC	BBC	ASTM[a]
Yield (wt.%)	40.70	25.05	ND
Moisture content (wt.%)	7.01	19.5	ND
Volatile matter (wt.%)	12.6	17.98	15–70%
Ash content (wt.%)	6.52	6.16	1–60%
Fixed carbon (wt.%)	74.4	56.36	ND
Element content by EDS (wt.%)			
C	80.74	73.91	ND
O	18.82	26.09	ND
Ca	0.43	–	ND
Textural properties			
Surface area (m^2/g)	6.32	73.95	ND
Pore volume (cc/g)	0.003	0.021	ND
Pore diameter (nm)	3.065	3.421	ND

[a]American Society for Testing and Materials.

The SEM images demonstrated significant alterations in the surface morphology of both varieties of biochar (CBC and BBC). As shown in Figure 2, the SEM images of both biochar varieties revealed a highly complex network of pores comprised of numerous channels of varying diameters (Shivakumar & Maitra 2020; Mansee *et al.* 2023). The CBC wall boundary structure became notably more specific and thicker than that of BBC; however, BBC contained a more significant number of the bigger pores depicted in Figure 2 Consequently, based on the SEM image, it was depicted that the adsorption mechanisms of two types of biochar are distinct. The biochar BBC adsorb azithromycin with the help of larger pores on the surface and CBC adsorb azithromycin with the help of small pores.

From the BET analysis (Supplementary material, Figure S2), the surface area of BBC (73.95 m^2/g) was higher than that of CBC (6.32 m^2/g). Here, pore formation may be due to the release of volatile components (Shikuku & Mishra 2021). The number of small pores present in CBC is more than in BBC, but the surface area was decreased due to the overlapping of pores in CBC (R and Maitra, 2020). Table 1 also illustrates the data from the EDS analysis. From the table, it is evident that carbon is the main component of the biochar. The oxygen in the biochar is from the functional groups containing oxygen, such as –COOH, and –OH (Zeng *et al.* 2018).

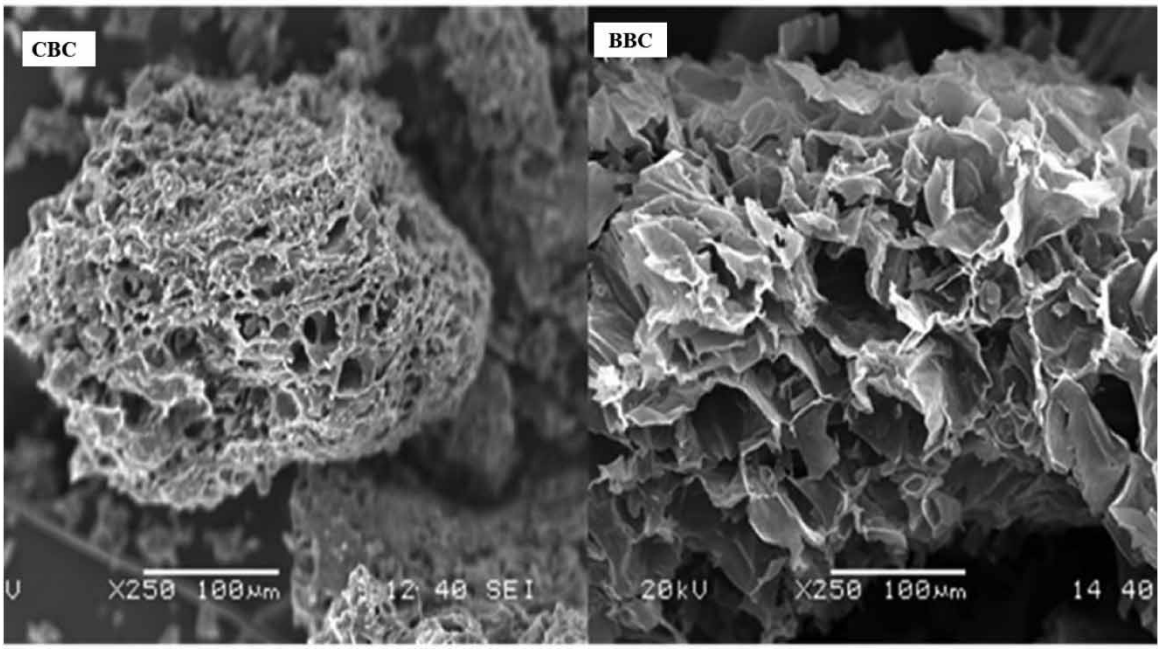

Figure 2 | SEM image of biochar (CBC) *T. chebula* biochar and (BBC) bagasse biochar.

Figure 3 represents the FTIR spectra for both the biochar. The bands at 3,400 cm^{-1} represent the O–H stretching vibrations, the band at 2,900 cm^{-1} represents the C–H stretching vibrations, the bands at 1,800 cm^{-1} and 1,700 cm^{-1} represent the C = O stretching vibrations, 1,450 cm^{-1} represents the –COOH vibrations and 800 cm^{-1} represent the bending vibrations and after adsorption of azithromycin both the biochar shows 2,650 and 2,639 cm^{-1} represents COOH vibration, 2,082 and 2,094 cm^{-1} represents C = C stretching vibration and 1,017–1,112 represents C–O–C stretching vibration (Garg *et al.* 2004; Liang *et al.* 2016). Peng *et al.* (2016) studied the adsorption of azithromycin by using spent mushroom substrate biochar, and the authors also observed an O–H stretching vibration band at 3,450 cm^{-1} (Peng *et al.* 2016). Upoma *et al.* (2022) also suggested that oxygen-containing functional groups on the adsorbent serve as active sites for the adsorption of azithromycin (Upoma *et al.* 2022). Therefore, in this study, the oxygen-containing functional groups (–OH, C = O, and –COOH) present on the surface of CBC and BBC enabled hydrogen bonding with azithromycin and were responsible for the adsorption.

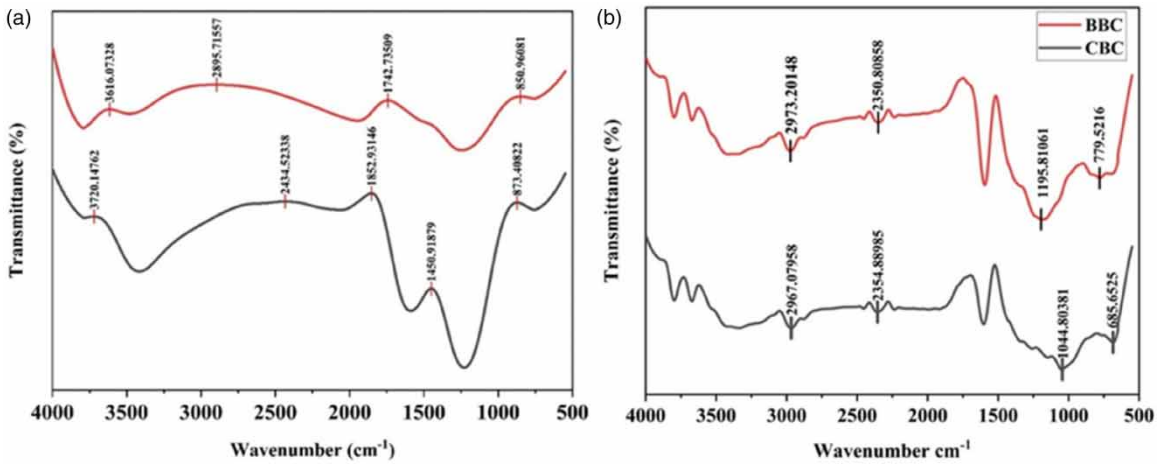

Figure 3 | FTIR spectra of biochar *T. chebula* biochar (CBC) and bagasse biochar (BBC). (a) Before adsorption and (b) after adsorption.

The XRD peak profile was observed for CBC and BBC, shown in Supplementary material, Figure S3. Both samples show a broad diffraction peak around 24°, which suggests both are amorphous in nature. Also, the hkl values for both the biochars are similar, i.e., (002) plane of the fabricated material, which diffuses a peak as graphite. Pandey *et al.* (2022b) studied the XRD pattern of pine needle for adsorption of Congo Red, and the pattern was similar to the current study i.e., 2Θ 24° and hkl as 002 (Pandey *et al.*, 2022b).

3.2. Adsorption studies

From the initial batch adsorption studies, it was observed that the adsorption reached equilibrium after 120 min. The percent azithromycin adsorbed was 32.21 and 28.82% for CBC and BBC, respectively. The optimization studies were carried out for 120 min. Table 2 gives the design matrix for the three process variables produced by the software, experimental and predicted data for the series of adsorption experiments conducted. The relation between the adsorption capacity and the independent process variables chosen by the CCD is given by the second-order polynomial equation (Bayuo *et al.* 2020). The R^2- value (correlation coefficient) for CBC and BBC was 94.31 and 96.01%, respectively, as established by the model (Mohan Kumar *et al.* 2013). Supplementary material, Table S1 gives the ANOVA results for both the biochar. The *P*-values for the individual and squared parameters are less than 0.05 which indicates that the results obtained are significant. The 3-D surface plot shows the effect of temperature and pH (Figure 4(a) and 4(d)), temperature and dosage (Figure 4(b) and (e)) and pH and Dosage (Figure 4(c) and 4(f)) on % of azithromycin adsorbed on biochar. The optimal conditions for CBC adsorption were a biochar dosage of 0.35 g, pH of 8.47 and temperature of 37.5 °C.

Table 2 | RSM design and the experimental and predicted results

	Parameters			CBC		BBC	
Run order	Dosage	pH	Temp.	% Adsorbed experimental	% Adsorbed predicted	% Adsorbed experimental	% Adsorbed predicted
1	0.2	5.5	28	13.43	12.83	7.93	10.3
2	0.4	5.5	28	6.64	11.78	4.41	4.82
3	0.2	9	28	16.86	17.51	1.32	2.4
4	0.4	9	28	27.57	29.09	0.44	3.84
5	0.2	5.5	36	19.36	18.89	7.34	6.61
6	0.4	5.5	36	22.53	22.94	16.99	18.59
7	0.2	9	36	25.61	21.53	12.36	14.62
8	0.4	9	36	36.53	38.19	33.23	33.52
9	0.132	7.25	32	5.025	8.21	9.82	8.13
10	0.468	7.25	32	26.03	21.34	21.52	19.4
11	0.3	4.31	32	15.97	13.81	12.08	11.19
12	0.3	10.19	32	29.93	30.58	20	17.1
13	0.3	7.25	25.27	27.11	23.62	1.3	−1.73
14	0.3	7.25	38.72	34.39	36.37	20.87	20.12
15	0.3	7.25	32	34.14	34.29	19.63	21.06
16	0.3	7.25	32	33.78	34.29	22.65	21.06
17	0.3	7.25	32	34.5	34.29	21.14	21.06
18	0.3	7.25	32	34.43	34.29	21.89	21.06
19	0.3	7.25	32	34.85	34.29	20.38	21.06
20	0.3	7.25	32	33.78	34.29	20	21.06

The three-dimensional response surface diagrams illustrate the interactive effect of two parameters on % adsorption while the other parameter is held at the center point (Figure 4). The interaction between pH and temperature was significant in the case of BBC ($p < 0.05$) and in the case of CBC it was not significant ($p > 0.05$) (Supplementary material, Table S1). From Figure 4(a), it was observed that the change in temperature did not

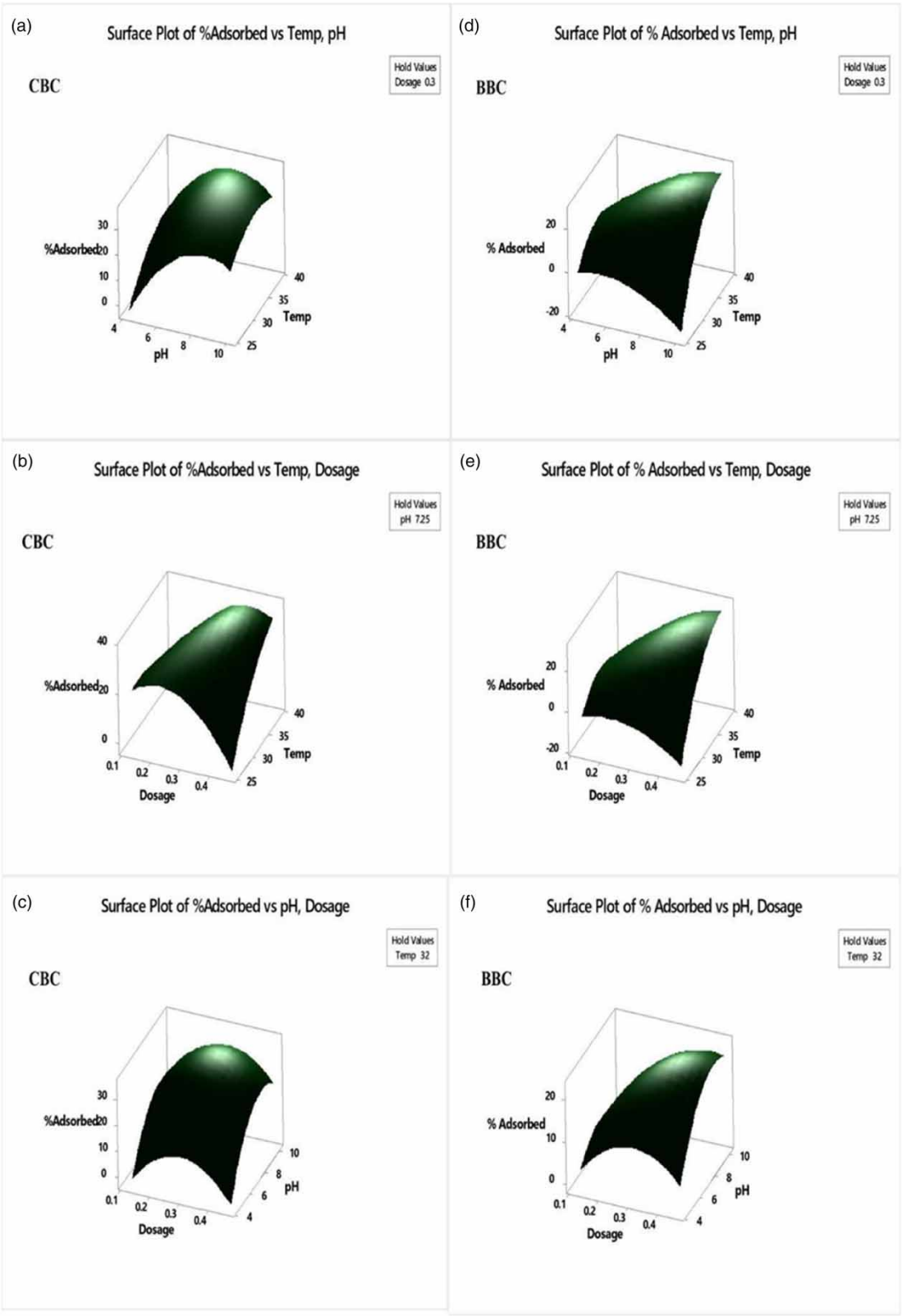

Figure 4 | Surface plots showing interactive effect of (a) and (d) pH and temperature; (b) and (e) dosage and temperature; (c) and (f) dosage and pH on azithromycin % Adosrbed for both CBC and BBC ($C_0 = 200$ mg/L, $V = 50$ mL, shaking speed = 160 rpm).

show any significant change in adsorption %. Whereas from Figure 4(d), it could be observed that a decrease in pH and an increase in temperature significantly improve the % adsorption. The interactive effect of dosage and temperature was found to be significant for BBC and insignificant for BBC (Table S1). From Figure 4(b) and 4(e),

it could be observed that an increase in dosage initially favored the adsorption process, however after the optimal condition, the increase in dosage negatively affected the adsorption process at low temperatures. An increase in temperature showed a positive impact on both the biochars. The interactive effect of pH and dosage was found to be significant for adsorption by CBC and insignificant in the case of BBC (Supplementary material, Table S1). The minimum adsorption was experienced at the highest and lowest levels of dosage for both the CBC and BBC (Figure 4(c) and 4(f)). Whereas the initial increase in pH improved the adsorption and reached the maximum. Further increase in pH lowered the % adsorption a little for both CBC and BBC.

The optimal conditions for BBC were a biochar dosage of 0.47 g, pH of 10.19 and temperature of 38.72 °C. Supplementary material, Table S2 gives the model summary for the CBC and BBC. Following optimization, the percentage of azithromycin adsorbed by CBC increased from 32.21 to 57.17%, whereas it increased from 28.82 to 60.03% for BBC. After optimization, adsorption increased by 1.77-fold in BBC and 2.08-fold in CBC (Table 3).

Table 3 | A comparison between the azithromycin adsorption before and after optimization

Azithromycin (200 mg/L)	Process variables	Before optimization	After optimization
CBC	Biochar dosage (g)	0.2	0.35
	pH	7	8.47
	Temperature (°C)	30	37.5
	Adsorption (%)	32.21	57.17
BBC	Biochar dosage (g)	0.2	0.47
	pH	7	10.19
	Temperature (°C)	30	38.72
	Adsorption (%)	28.82	60.03

3.3. Adsorption kinetics studies

To understand the adsorption kinetics of azithromycin on CBC and BBC, adsorption experiments were conducted at concentrations varying from 100 to 400 mg/L with a time interval of 30 min. The pseudo-first and second-order kinetics models were used to correlate the experimental data. Figures 5 and 6 depict the linear and nonlinear pseudo-first- and pseudo-second-order model fitting curves, respectively. It was observed that the calculated q_e (mg/g) values from nonlinear pseudo-first-order model for CBC (8.58–21.33) and BBC (7.04–17.14) were close to the experimental values (CBC: 9.16–20.34 mg/g; for BBC 7.38–16.85 mg/g) (Supplementary material, Table S3). The nonlinear model helps to predict the q_e value directly from the course of adsorption over time but is difficult to obtain in linear pseudo-first-order (Lagergren 1898; López *et al.* 2019).

3.4. Adsorption isotherm studies

To explore the adsorption mechanism and its effectiveness of the generated biochar, experimental data from the adsorption kinetics study was utilized to fit the adsorption isotherm models (Ayawei *et al.*, 2017). In Figure 7, the fitting curves for the adsorption isotherm are given. Supplementary material, Table S4 gives the parameters for the adsorption isotherm models. The R^2 values for the Langmuir model for CBC and BBC are 0.88 and 0.87, respectively, indicating a better fit when compared to other models (Langmuir *et al.* 1919). Stylianou *et al.* (2021) studied the removal of seven antibiotics using organic waste feedstock as a biochar, and in their study, the Freundlich model was properly fitted with R^2 values of 0.87–0.96 (Stylianou *et al.* 2021). Li *et al.* (2019) studied antibiotic adsorption using biochar and concluded that for tetracycline adsorption at different conditions, the adsorption Langmuir model had an R^2 value range of 0.85–0.99 (Li *et al.* 2019). This can be said to be accurate from previous studies of antibiotic adsorption on biochar (Fan *et al.* 2021; Ho 2006). The value of $R_L < 1$ indicates that azithromycin was effective on both biochars. Also, it is evident from the BET analysis that the adsorbent is relatively non-porous and here Langmuir model of both biochars suggests that azithromycin formed a monolayer. The maximum monolayer adsorption capacities of CBC and BBC were 21.36 and 17.95 mg/g, respectively.

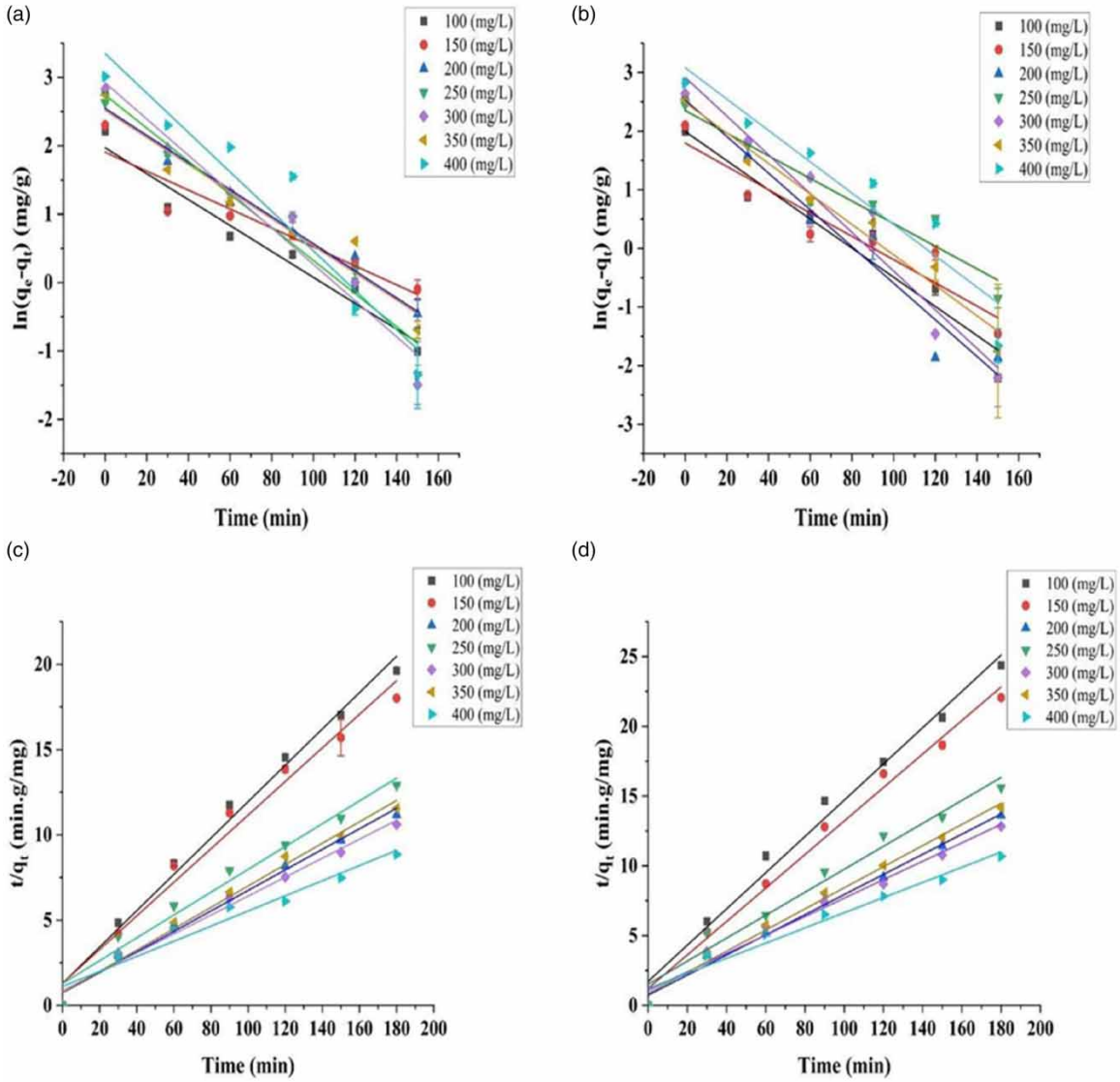

Figure 5 | Adsorption kinetics plot: linear pseudo-first-order (a) CBC, (b) BBC; linear pseudo-second-order (c) CBC, (d) BBC (C0 = 100–400 mg L, V = 50 mL, adsorbent dosage = 0.35 g(CBC); 4.7 g(BBC), pH 8.47(CBC); 10.19(BBC), temperature = 37.5 °C (CBC); 38.7 °C (BBC), shaking speed = 160 rpm).

3.5. Thermodynamic analysis

Thermodynamic studies were performed to analyze the change in energy of the experiment, as shown in Table 4 and Supplementary material, Figures S4 and S5. In both biochars, the free energy ΔG value is negative and decreases with increasing temperature, which implies that the adsorption process involved is spontaneous and feasible. The azithromycin adsorption on both the biochar is an exothermic reaction and is evident by the negative value of ΔH. Bagasse ΔH is −20.06 kJ/mol, while for *T. chebula* ΔH is −14.89 kJ/mol, suggesting that bagasse adsorbs more energy than *T. chebula* for azithromycin adsorption. The stability and unpredictability of the adsorption process are indicated by the positive values of ΔS (Pandey *et al.*, 2022a; Yao *et al.* 2020). Even though the drug has three degrees of freedom in the fluid phase and after adsorption, it loses one degree of freedom, therefore, the system is ordered. However, the entropy change of the entire process remains positive. The total entropy of the system is comprised of the total entropy of azithromycin and its surroundings. Theoretically, the entropy of azithromycin decreases because of a reduction in the degree of freedom however the entropy change was found positive. This rise in the entropy of the system must have been due to a rise in the entropy of the surroundings. *ln K* was plotted against 1/T, ΔH, and ΔS were calculated from the slope and intercept, respectively (see Supplementary material, Figures S4 and S5). Similar results have also been observed by (Ebisike *et al.*, 2023), where adsorption was spontaneous and exothermic.

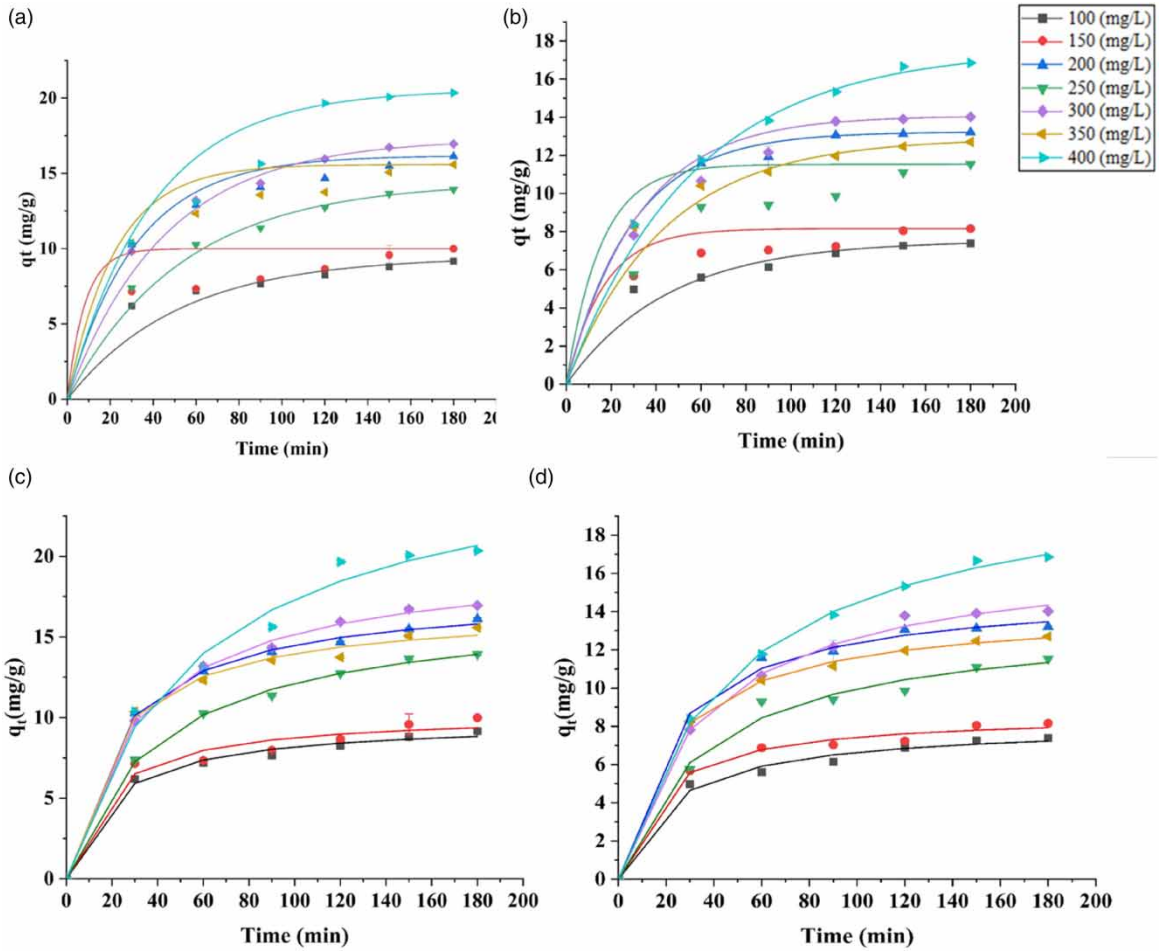

Figure 6 | Adsorption kinetics plot: nonlinear pseudo-first-order (a) CBC, (b) BBC; nonlinear pseudo-second-order (c) CBC, (d) BBC (C_0 = 100–400 mg/L, V = 50 mL, adsorbent dosage = 0.35 g (CBC); 4.7 g(BBC), pH 8.47(CBC); 10.19(BBC), temperature = 37.5 °C (CBC); 38.7 °C (BBC), shaking speed = 160 rpm).

3.6. Reusability of CBC and BBC

Reusability studies of sorbents are critical for their commercial applications. Figure 8 shows the azithromycin removal efficiencies of CBC and BBC after three recycled generations. The outcomes demonstrated the ability of both forms of biochar to regenerate, although the removal rate fell with each cycle because of the loss or obstruction of adsorption sites. In comparison to the CBC, the BBC was shown to have a greater potential for commercial use as a low-cost adsorbent since it continued to remove a larger proportion of azithromycin after three cycles. These results indicate that biochar can be a cost-efficient and long-lasting material for removing antibiotics from wastewater and that future studies should concentrate on optimizing the regeneration process to increase the durability and effectiveness of the adsorbent.

3.7. Mechanism of interaction of CBC and BBC with azithromycin

Various mechanisms such as hydrogen bonding, electrostatic interaction, and pore-filling have been involved in the interaction between the biochar and azithromycin (Figure 9).

3.7.1. Hydrogen bonding

Azithromycin comprises functional groups, including hydroxyl and carbonyl groups, which are capable of forming hydrogen bonds with the biochar. The surface interactions enhance the adsorption and retention of azithromycin on biochar. FTIR data further confirm the presence of hydroxyl, carboxylic acid, alkyl, and carbonyl groups which facilitate the formation of H-bond on the surface of BBC and CBC (Guo *et al.* 2023).

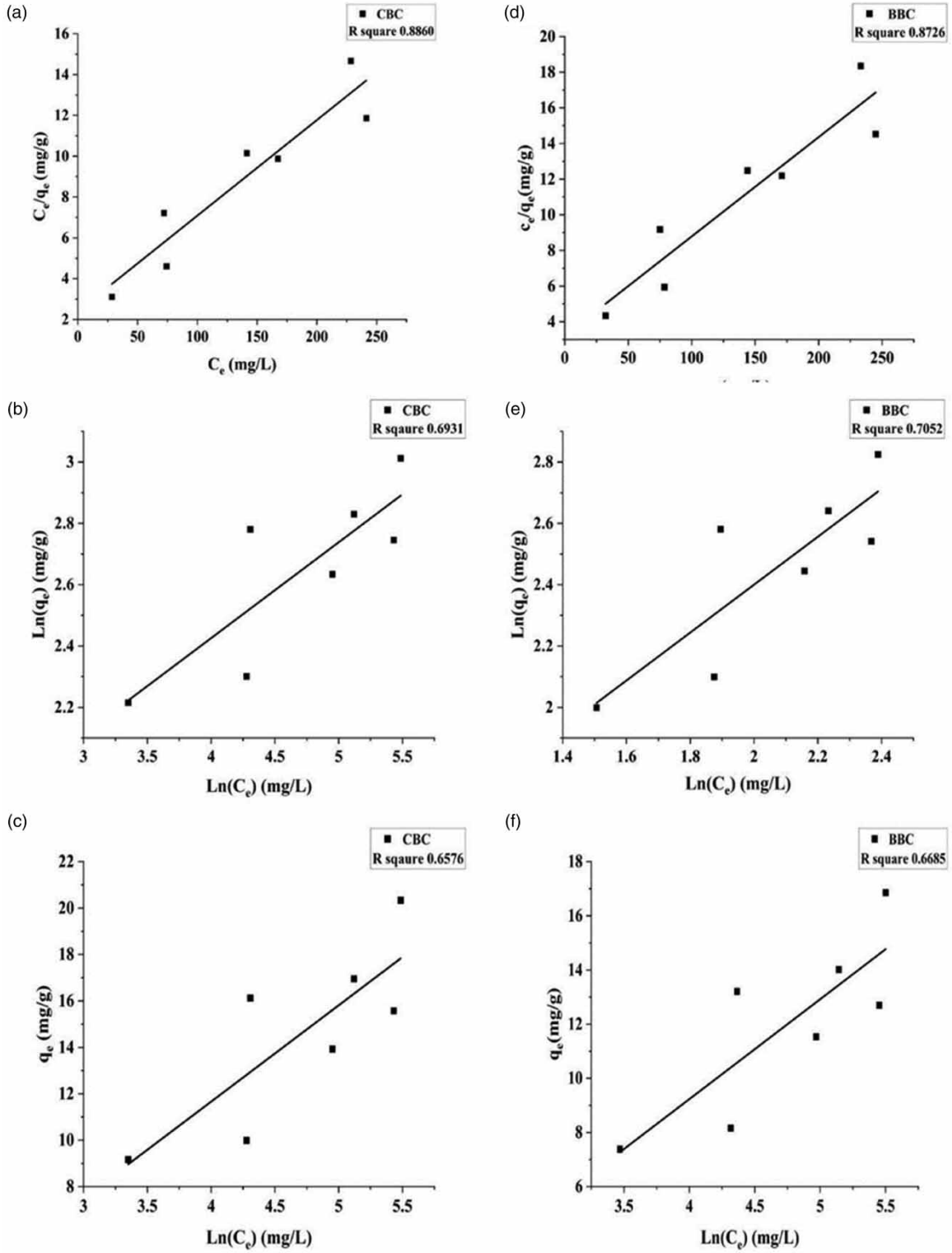

Figure 7 | Adsorption isotherm plots (a), (d) Langmuir; (b), (e) Freundlich; (c), (f) Temkin; Halsey (g), (i); Elvonich (h), (j). (Co = 100–400 mg L^{-1}, V = 50 mL, shaking speed = 160 rpm). (*continued.*).

3.7.2. Electrostatic interaction

The adsorption process of azithromycin and biochar can be aided by the electrostatic attraction between their charged groups. In the case of both the biochar (CBC and BBC) depicts the electrostatic interaction by FTIR analysis. The bond intensity was higher in CBC than in BBC. The adsorption of azithromycin by biochar was

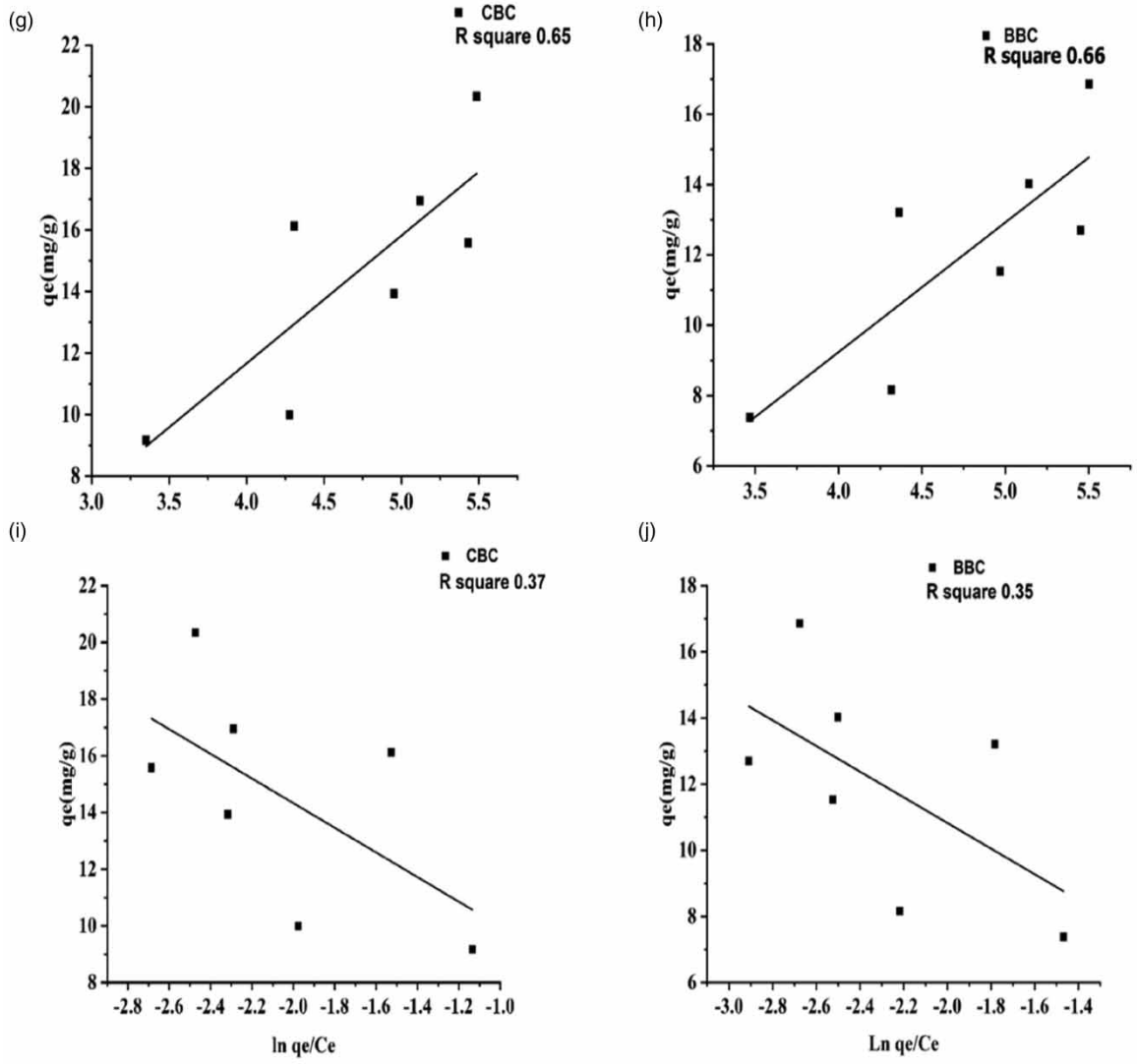

Figure 7 | Continued.

Table 4 | Thermodynamic for removal efficiency

Temperature (°C)	Concentration of azithromycin	*K*	Δ*G* (kJ/mol)	Δ*H* (kJ/mol)	Δ*S* (kJ/mol K)
T. chebula biochar					
29.9	262.29	0.08	−8,742.23	− 14.89	28.80
37.3	240.50	0.09	−8,958.26		
43.9	221.21	0.11	−9,145.48		
Sugarcane bagasse biochar					
29.9	276.57	0.07	−13,635.45	− 20.06	44.93
37.3	247.64	0.09	−14,027.28		
43.9	224.07	0.1	−14,264.54		

also done by electrostatic induction mechanism because the charge present on the surface of azithromycin was neutral (Upoma *et al.* 2022) and negative in the biochar surface. The negative charge of the biochar was confirmed by the Pzc analysis, desorption and optimum pH obtained during the optimization study (Dong *et al.* 2024).

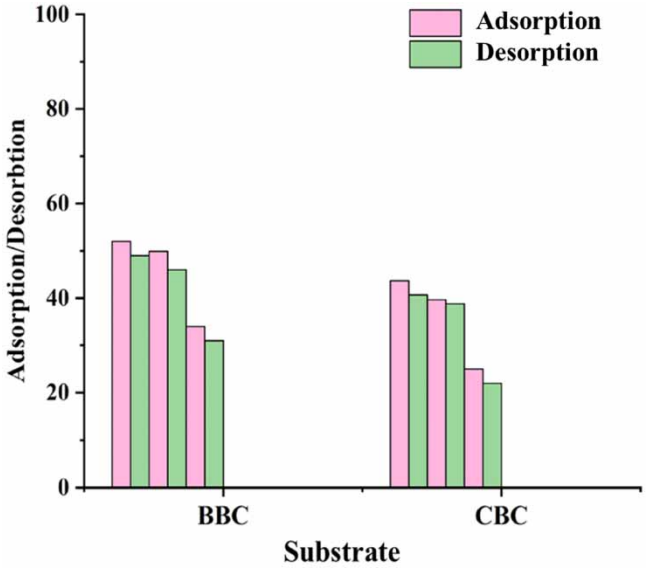

Figure 8 | Desorption and adsorption studies of CBC and BBC.

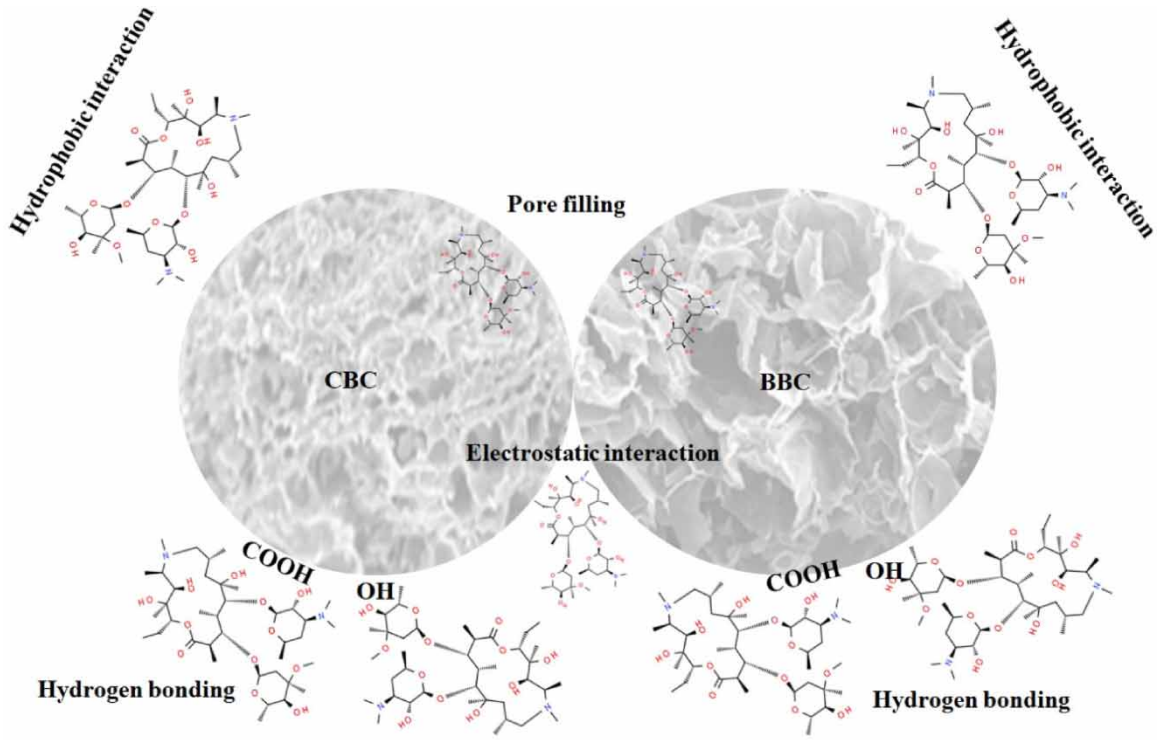

Figure 9 | A schematic representation for the mechanism of azithromycin (neutral charge) adsorption on CBC and BBC biochar (negative charge).

3.7.3. Pore-filling

Biochar usually has a porous structure, as confirmed by the data obtained by SEM and BET analysis. More surface area contacts and a longer period of antibiotic release result from azithromycin molecules entering and filling the pores.

3.7.4. Hydrophobic interaction

The presence of nonpolar groups confirmed by the FTIR analysis of both the biochar (C = O, O–H and C–H) interact to form anhydrous domain in aqueous solution that facilitates adsorption of azithromycin on the biochar (Ambaye *et al.* 2021; Mansee *et al.* 2023).

Table 5 | Meta-analysis of azithromycin adsorption

Biochar/Biosorbent	Azithromycin concentration (mg/L)	Removal efficiency	References
Rice husk	200	95	Herrera *et al.* (2022)
Tanner hair waste	100	94	Herrera *et al.* (2023)
$CoFe_2O_4$/NiO nanoparticles anchored onto the porous activated carbon (N-PAC)	20	96.25	Ameen *et al.* (2023)
Saponin-modified nano diatomite	100	95	Davoodi *et al.* (2019)
CBC	200	57.17	This study
BBC	200	60.03	

4. CONCLUSION

The biochar was successfully prepared from the *T. chebula* fruits and sugarcane bagasse. After optimizing biochar dosage, pH, and temperature, both CBC and BBC could absorb (about 60%) of azithromycin from water. The meta-analysis (Table 5) of azithromycin adsorption also confirms the maximum 200 mg/L of concentration was carried out using biochar. The Langmuir model was best fitted among the tested isotherm models for both types of biochar. The thermodynamic study suggests that the process was spontaneous and feasible, ΔH was exothermic and ΔS has shown stability and unpredictability for azithromycin adsorption. The yield of CBC was found to be 1.6-fold greater than the yield of BBC. The reproducibility of the BBC was more than CBC suggesting its high reusability. The study concluded that the pristine CBC and BBC both showed better adsorption for azithromycin from water. After optimizing biochar dosage, pH, and temperature, for both CBC and BBC the removal efficiencies of ~60% may be too low to be economically feasible. Further, the adsorption of azithromycin on the CBC and BBC can be improved by modifying the biochar and their potential with real wastewater need to be tested in future.

ACKNOWLEDGEMENT

The authors would like to thank NIT Rourkela for institute funding and Institute's Central Research Facility (CRF) access.

AUTHORS' CONTRIBUTIONS

M.P. conducted experiments and collected data, analyzed samples and data, wrote the draft, reviewed and edited the article. S.S. analyzed data, wrote the draft, reviewed and edited the article. D.K. analyzed data, wrote the draft, reviewed and edited the article. A.D. conceptualized the study, wrote the draft, reviewed and edited the article. K.D. conceptualized, supervised, wrote the draft, reviewed and edited the article, collected funds.

FUNDING

The authors would like to thank NIT Rourkela for providing institute funding to carry out this work.

DATA AVAILABILITY STATEMENT

All relevant data are included in the paper or its Supplementary Information.

CONFLICT OF INTEREST

The authors declare there is no conflict.

REFERENCES

Ambaye, T. G., Vaccari, M., van Hullebusch, E. D., Amrane, A. & Rtimi, S. 2021 Mechanisms and adsorption capacities of biochar for the removal of organic and inorganic pollutants from industrial wastewater. *International Journal of Environmental Science and Technology* **18**, 3273–3294. https://doi.org/10.1007/s13762-020-03060-w.

Ameen, F., Mostafazadeh, R., Hamidian, Y., Erk, N., Sanati, A. L., Karaman, C. & Ayati, A. 2023 Modeling of adsorptive removal of azithromycin from aquatic media by $CoFe_2O_4$/NiO anchored microalgae-derived nitrogen-doped porous activated carbon adsorbent and colorimetric quantifying of azithromycin in pharmaceutical products. *Chemosphere* **329**, 138635. https://doi.org/10.1016/j.chemosphere.2023.138635.

Ayawei, N., Ebelegi, A. N. & Wankasi, D. 2017 Modelling and interpretation of adsorption isotherms. *Journal of Chemistry* **2017**, 1–11. https://doi.org/10.1155/2017/3039817.

Bayuo, J., Abukari, M. A. & Pelig-Ba, K. B. 2020 Optimization using central composite design (CCD) of response surface methodology (RSM) for biosorption of hexavalent chromium from aqueous media. *Applied Water Science* **10**, 1–12. https://doi.org/10.1007/s13201-020-01213-3.

Chen, Y., Shi, J., Du, Q., Zhang, H. & Cui, Y. 2019 Antibiotic removal by agricultural waste biochars with different forms of iron oxide. *RSC Advances* **9**, 14143–14153. https://doi.org/10.1039/c9ra01271k.

Dadgostar, P. 2019 Antimicrobial resistance: Implications and costs. *Infection and Drug Resistance* **12**, 3903–3910. https://doi.org/10.2147/IDR.S234610.

Davoodi, S., Dahrazma, B., Goudarzi, N. & Gorji, H. G. 2019 Adsorptive removal of azithromycin from aqueous solutions using raw and saponin-modified nano diatomite. *Water Science and Technology* **80**, 939–949. https://doi.org/10.2166/wst.2019.337.

Dong, X., Chu, Y., Tong, Z., Sun, M., Meng, D., Yi, X., Gao, T., Wang, M. & Duan, J. 2024 Mechanisms of adsorption and functionalization of biochar for pesticides: A review. *Ecotoxicology and Environmental Safety* **272**, 116019. https://doi.org/10.1016/J.ECOENV.2024.116019.

Ebisike, K., Okoronkwo, A. E., Alaneme, K. K. & Akinribide, O. J. 2023 Thermodynamic study of the adsorption of Cd^{2+} and Ni^{2+} onto chitosan – Silica hybrid aerogel from aqueous solution. *Results in Chemistry* **5**, 100730. https://doi.org/10.1016/j.rechem.2022.100730.

Fan, X., Qian, Z., Liu, J., Geng, N., Hou, J. & Li, D. 2021 Investigation on the adsorption of antibiotics from water by metal loaded sewage sludge biochar. *Water Science and Technology* **83**, 739–750. https://doi.org/10.2166/wst.2020.578.

Garg, V. K., Gupta, R., Kumar, R. & Gupta, R. K. 2004 Adsorption of chromium from aqueous solution on treated sawdust. *Bioresource Technology* **92**, 79–81. https://doi.org/10.1016/j.biortech.2003.07.004.

Guo, S., Zou, Z., Chen, Y., Long, X., Liu, M., Li, X., Tan, J. & Chen, R. 2023 Synergistic effect of hydrogen bonding and π-π interaction for enhanced adsorption of rhodamine B from water using corn straw biochar. *Environmental Pollution* **320**, 121060. https://doi.org/10.1016/J.ENVPOL.2023.121060.

Herrera, K., Morales, L. F., Tarazona, N. A., Aguado, R. & Saldarriaga, J. F. 2022 Use of biochar from rice husk pyrolysis: Part A: Recovery as an adsorbent in the removal of emerging compounds. *ACS Omega* **7**, 7625–7637. https://doi.org/10.1021/acsomega.1c06147.

Herrera, K., Morales, L. F., López, J. E., Montoya-Ruiz, C., Muñoz, S., Zapata, D. & Saldarriaga, J. F. 2023 Biochar production from tannery waste pyrolysis as a circular economy strategy for the removal of emerging compounds in polluted waters. *Biomass Conversion and Biorefinery*, pp. 1–14. https://doi.org/10.1007/s13399-023-04261-2.

Ho, Y. S. 2006 Review of second-order models for adsorption systems. *Journal of Hazardous Materials* **136**, 681–689. https://doi.org/10.1016/j.jhazmat.2005.12.043.

Iwuozor, K. O., Chizitere Emenike, E., Ighalo, J. O., Omoarukhe, F. O., Omuku, P. E. & George Adeniyi, A. 2022 A review on the thermochemical conversion of sugarcane bagasse into biochar. *Cleaner Materials* **6**, 100162. https://doi.org/10.1016/j.clema.2022.100162.

Jacob, M. M., Ponnuchamy, M., Kapoor, A. & Sivaraman, P. 2020 Bagasse based biochar for the adsorptive removal of chlorpyrifos from contaminated water. *Journal of Environmental Chemical Engineering* **8**, 103904. https://doi.org/10.1016/j.jece.2020.103904.

Koch, D. E., Bhandari, A., Close, L. & Hunter, R. P. 2005 Azithromycin extraction from municipal wastewater and quantitation using liquid chromatography/mass spectrometry. *Journal of Chromatography A* **1074**, 17–22. https://doi.org/10.1016/j.chroma.2005.03.052.

Kumar, V., Singh, S. K., Gulati, M., Anishetty, R. & Shunmugaperumal, T. 2013 Development and validation of a simple and sensitive spectrometric method for estimation of azithromycin dihydrate in tablet dosage forms: Application to dissolution studies. *Current Pharmaceutical Analysis* **9**, 310–317. https://doi.org/10.2174/1573412911309030009.

Kwoczynski, Z. & Čmelík, J. 2021 Characterization of biomass wastes and its possibility of agriculture utilization due to biochar production by torrefaction process. *Journal of Cleaner Production* **280**, 124302. https://doi.org/10.1016/j.jclepro.2020.124302.

Lagergren, S. 1898 About the theory of So-called adsorption of soluble substances. *Sven. Vetenskapsakad. Handingarl.* **24**, 1–39.

Langmuir, I. 1919 Diminishing approximately 1% for. *Journal of the American Chemical Society* **40**, 1361–1403.

Li, C., Zhu, X., He, H., Fang, Y., Dong, H., Lü, J., Li, J. & Li, Y. 2019 Adsorption of two antibiotics on biochar prepared in air-containing atmosphere: Influence of biochar porosity and molecular size of antibiotics. *Journal of Molecular Liquids* **274**, 353–361. https://doi.org/10.1016/j.molliq.2018.10.142.

Liang, H., Chen, L., Liu, G. & Zheng, H. 2016 Surface morphology properties of biochars produced from different feedstocks 1205–1208. https://doi.org/10.2991/iccte-16.2016.210.

López, J., Loida, L., Montes, E. R., Martinez, S. & Arturo, V. 2019 Linear and nonlinear kinetic and isotherm adsorption models for arsenic removal by manganese ferrite nanoparticles. *SN Applied Sciences* **1**, 1–19. https://doi.org/10.1007/s42452-019-0977-3.

Mahecha-Rivas, J. C., Fuentes-Ordoñez, E., Epelde, E. & Saldarriaga, J. F. 2021 Aluminum extraction from a metallurgical industry sludge and its application as adsorbent. *Journal of Cleaner Production* **310**, 1–11. https://doi.org/10.1016/j.jclepro.2021.127374.

Mangal, S., Nie, H., Xu, R., Guo, R., Cavallaro, A., Zemlyanov, D. & Zhou, Q. 2018 Physico-chemical properties, aerosolization and dissolution of co-spray dried azithromycin particles with l-leucine for inhalation. *Pharmaceutical Research* **35**, 1–15.

Mansee, A. H., Abdelgawad, D. M., El-Gamal, E. H., Ebrahim, A. M. & Saleh, M. E. 2023 Influences of Mg-activation on sugarcane bagasse biochar characteristics and its PNP removing potentials from contaminated water. *Scientific Reports* **13**, 1–17. https://doi.org/10.1038/s41598-023-46463-8.

Marston, H., Dixon, D., Knisel, M., Palmore, T. & Fauci, A. 2016 Los agentes antimicrobianos modificados y las intervenciones de salud pública junto con nuevas estrategias antimicrobianas pueden ayudar a mitigar el efecto de los organismos multirresistentes. *Intramed* **316**, 14.

Masrura, S. U., Jones-Lepp, T. L., Kajitvichyanukul, P., Ok, Y. S., Tsang, D. C. W. & Khan, E. 2022 Unintentional release of antibiotics associated with nutrients recovery from source-separated human urine by biochar. *Chemosphere* **299**, 134426. https://doi.org/10.1016/j.chemosphere.2022.134426.

Mdlalose, L. M. 2018 The synthesis, characterization and performance evaluation of polyphenylenediamine- and polypyrrole-clay composites for removal of oxo-anionic wastewater contaminants 167.

Mohan Kumar, K., Mandal, B. K., Siva Kumar, K., Sreedhara Reddy, P. & Sreedhar, B. 2013 Biobased green method to synthesise palladium and iron nanoparticles using Terminalia chebula aqueous extract. *Spectrochimica Acta Part A: Molecular and Biomolecular Spectroscopy* **102**, 128–133. https://doi.org/10.1016/j.saa.2012.10.015.

Muter, O., Pērkons, I. & Bartkevičs, V. 2019 Removal of pharmaceutical residues from wastewater by woodchip-derived biochar. *Desalination Water Treat* **159**, 110–120. https://doi.org/10.5004/dwt.2019.24108.

Nallathambi, G., Surendra Kumar, M., Meganthiya, D., Jayapriya, R., Dinesh, V., Nareshkumar, A. & Akash, A. 2022 Overview on Terminalia Chebula Retz. *International Journal of Pharmaceutical Research and Applications* **7**, 1250–1258. https://doi.org/10.35629/7781-070412501258.

Pan, M. 2020 Biochar adsorption of antibiotics and its implications to remediation of contaminated soil. *Water, Air & Soil Pollution* **231**, 221. https://doi.org/10.1007/s11270-020-04551-9.

Pandey, D., Daverey, A. & Arunachalam, K. 2020 Biochar: Production, properties and emerging role as a support for enzyme immobilization. *Journal of Cleaner Production* **255**, 120267. https://doi.org/10.1016/j.jclepro.2020.120267.

Pandey, D., Daverey, A., Dutta, K., Yata, V. K. & Arunachalam, K. 2022a Valorization of waste pine needle biomass into biosorbents for the removal of methylene blue dye from water: Kinetics, equilibrium and thermodynamics study. *Environmental Technology & Innovation* **25**, 102200. https://doi.org/10.1016/j.eti.2021.102200.

Pandey, D., Daverey, A., Dutta, K. & Arunachalam, K. 2022b Enhanced adsorption of Congo red dye onto polyethyleneimine-impregnated biochar derived from pine needles. *Environmental Monitoring and Assessment* **194**(12), 880. https://doi.org/10.1007/s10661-022-10563-1.

Peng, B., Chen, L., Que, C., Yang, K., Deng, F., Deng, X., Shi, G., Xu, G. & Wu, M. 2016 Adsorption of antibiotics on graphene and biochar in aqueous solutions induced by π-π interactions. *Scientific Reports* **6**, 1–10. https://doi.org/10.1038/srep31920.

Peng, Z., Hu, Z., Li, Z., Zhang, X., Jia, C., Li, T., Dai, M., Tan, C., Xu, Z., Wu, B., Chen, H. & Wang, X. 2022 Antimicrobial resistance and population genomics of multidrug-resistant *Escherichia coli* in pig farms in mainland China. *Nature Communications* **13**, 1–11. https://doi.org/10.1038/s41467-022-28750-6.

Saldarriaga, J. F., Montoya, N. A., Estiati, I., Aguayo, A. T., Aguado, R. & Olazar, M. 2021 Unburned material from biomass combustion as low-cost adsorbent for amoxicillin removal from wastewater. *Journal of Cleaner Production* **284**, 124732. https://doi.org/10.1016/j.jclepro.2020.124732.

Shao, F., Zhang, X., Sun, X. & Shang, J. 2021 Antibiotic removal by activated biochar: Performance, isotherm, and kinetic studies. *Journal of Dispersion Science and Technology* **42**, 1274–1285. https://doi.org/10.1080/01932691.2020.1737106.

Sharma, R., Sikka, J., Bajpai, N. & Waghela, D. 2012 Impact of domestic sewage and industrial effluent on water quality of the Khan river, Indore (India). *Pollution Research* **31**, 289–296.

Shikuku, V. O. & Mishra, T. 2021 Adsorption isotherm modeling for methylene blue removal onto magnetic kaolinite clay: A comparison of two-parameter isotherms. *Applied Water Science* **11**, 1–9. https://doi.org/10.1007/s13201-021-01440-2.

Shivakumar, K. & Maitra, S. 2020 Evaluation of pore size and surface morphology during devolatilization of coconut fiber and sugarcane bagasse. *Combustion Science and Technology* **192**, 2326–2344. https://doi.org/10.1080/00102202.2019.1645655.

Singh, B., Dolk, M. M., Shen, Q. & Camps-Arbestain, M. 2017 Biochar pH, electrical conductivity and liming potential. In: *Biochar: A Guide to Analytical Methods* (Singh, B., Camps-Arbestain, M. & Lehman, J. eds.). CSIRP Australia, 23 pp. 23–38.

Stylianou, M., Christou, A., Michael, C., Agapiou, A., Papanastasiou, P. & Fatta-Kassinos, D. 2021 Adsorption and removal of seven antibiotic compounds present in water with the use of biochar derived from the pyrolysis of organic waste feedstocks. *Journal of Environmental Chemical Engineering* **9**, 105868. https://doi.org/10.1016/j.jece.2021.105868.

Tran, H. N., You, S. J. & Chao, H. P. 2016 Effect of pyrolysis temperatures and times on the adsorption of cadmium onto orange peel derived biochar. *Waste Management & Research* **34**, 129–138. https://doi.org/10.1177/0734242X15615698.

Upoma, B. P., Yasmin, S., Ali Shaikh, M. A., Jahan, T., Haque, M. A., Moniruzzaman, M. & Kabir, M. H. 2022 A fast adsorption of azithromycin on waste-product-derived graphene oxide induced by H-bonding and electrostatic interactions. *ACS Omega* **7**, 29655–29665. https://doi.org/10.1021/acsomega.2c01919.

William Kajjumba, G., Emik, S., Öngen, A., Kurtulus Özcan, H. & Aydın, S. 2019 Modelling of adsorption kinetic processes – errors, theory and application. In: *Advanced Sorption Process Application* (Edebali, S., ed). pp. 1–19. https://doi.org/10.5772/intechopen.80495.

Xu, D., Gao, Y., Lin, Z., Gao, W., Zhang, H., Karnowo, K., Hu, X., Sun, H., Syed-Hassan, S. S. A. & Zhang, S. 2020 Application of biochar derived from pyrolysis of waste fiberboard on tetracycline adsorption in aqueous solution. *Frontiers in Chemistry* **7**, 1–11. https://doi.org/10.3389/fchem.2019.00943.

Yao, X., Ji, L., Guo, J., Ge, S., Lu, W., Cai, L., Wang, Y., Song, W. & Zhang, H. 2020 Magnetic activated biochar nanocomposites derived from wakame and its application in methylene blue adsorption. *Bioresource Technology* **302**, 122842. https://doi.org/10.1016/j.biortech.2020.122842.

Zeng, Z. W., Tan, X. F., Liu, Y. G., Tian, S. R., Zeng, G. M., Jiang, L. H., Liu, S. B., Li, J., Liu, N. & Yin, Z. H. 2018 Comprehensive adsorption studies of doxycycline and ciprofloxacin antibiotics by biochars prepared at different temperatures. *Frontiers in Chemistry* **6**, 1–11. https://doi.org/10.3389/fchem.2018.00080.

First received 8 September 2023; accepted in revised form 16 May 2024. Available online 30 May 2024